Draft version October 19, 2021
Typeset using LaTeX **twocolumn** style in AASTeX63

Domains of Magnetic Pressure Balance in Parker Solar Probe Observations of the Solar Wind

David Ruffolo,[1] Nawin Ngampoopun,[1] Yash R. Bhora,[2] Panisara Thepthong,[3] Peera Pongkitiwanichakul,[3] William H. Matthaeus,[4,5] and Rohit Chhiber[4,6]

[1] *Department of Physics, Faculty of Science, Mahidol University, Bangkok 10400, Thailand*
[2] *Wells International School, Bangkok 10260, Thailand*
[3] *Department of Physics, Faculty of Science, Kasetsart University, Bangkok 10900, Thailand*
[4] *Department of Physics and Astronomy, University of Delaware, Newark, DE 19716, USA*
[5] *Bartol Research Institute, University of Delaware, Newark, DE 19716, USA*
[6] *Heliophysics Science Division, NASA Goddard Space Flight Center, Greenbelt MD 20771, USA*

(Accepted by the Astrophysical Journal, 2021 Oct 10)

ABSTRACT

The *Parker Solar Probe (PSP)* spacecraft is performing the first *in situ* exploration of the solar wind within 0.2 au of the Sun. Initial observations confirmed the Alfvénic nature of aligned fluctuations of the magnetic field **B** and velocity **V** in solar wind plasma close to the Sun, in domains of nearly constant magnetic field magnitude $|\mathbf{B}|$, i.e., approximate magnetic pressure balance. Such domains are interrupted by particularly strong fluctuations, including but not limited to radial field (polarity) reversals, known as switchbacks. It has been proposed that nonlinear Kelvin-Helmholtz instabilities form near magnetic boundaries in the nascent solar wind leading to extensive shear-driven dynamics, strong turbulent fluctuations including switchbacks, and mixing layers that involve domains of approximate magnetic pressure balance. In this work we identify and analyze various aspects of such domains using data from the first five *PSP* solar encounters. The filling fraction of domains, a measure of Alfvénicity, varies from median values of 90% within 0.2 au to 38% outside 0.9 au, with strong fluctuations. We find an inverse association between the mean domain duration and plasma β. We examine whether the mean domain duration is also related to the crossing time of spatial structures frozen into the solar wind flow for extreme cases of the aspect ratio. Our results are inconsistent with long, thin domains aligned along the radial or Parker spiral direction, and compatible with isotropic domains, which is consistent with prior observations of isotropic density fluctuations or "flocculae" in the solar wind.

1. INTRODUCTION

Fluctuating magnetic fields are prevalent in space plasmas. In the solar wind, such fluctuations play a key role in the acceleration (Drury 1983) and transport (Jokipii 1966) of energetic charged particles, including solar energetic particles, which are an important component of space weather effects of solar storms on human activity (Knipp 2011). Indeed, irregular magnetic fields in the heliosphere were initially inferred from the transport of relativistic solar ions (Sittkus 1956; Meyer et al. 1956), before the solar wind itself was proposed theoretically (Parker 1958) and confirmed observationally (Gringauz et al. 1960; Neugebauer & Snyder 1962). Magnetic fluctuations, together with velocity fluctuations, are often found as part of a turbulent cascade in space plasmas, and such turbulence has a significant impact on the large-scale properties of the solar wind flow (Usmanov et al. 2009; Kryukov et al. 2012; Wiengarten et al. 2015; Shiota et al. 2017). The solar wind also provides a natural laboratory for *in situ* studies of the nonlinear dynamics of large-amplitude waves and turbulence (Barnes 1979; Bruno & Carbone 2013). Here we will examine statistical properties of spatial regions, or domains, that have nearly constant magnetic field magnitude, using *Parker Solar Probe* datasets. As we shall presently elaborate upon, these domains have special relationships both to Alfvénic turbulence and to dynamical plasma relaxation processes. Consequently the statistics of these domains of nearly constant field magnitude may play an important role in understanding the nature and dynamics of the solar wind.

Corresponding author: David Ruffolo
david.ruf@mahidol.ac.th

Using observations of the solar wind from the *Mariner 5* mission from Earth to Venus, before and after its Venus flyby, Belcher & Davis (1971) reported that fluctuations in magnetic and velocity fields were largely consistent with Alfvén modes, satisfying the Walén relation (Walén 1944)

$$\mathbf{v} = \pm \frac{\mathbf{b}}{\sqrt{\mu_0 \rho}} \tag{1}$$

(as expressed for isotropic plasma pressure), where $\mathbf{v} \equiv \mathbf{V} - \mathbf{V}_0$ and $\mathbf{b} \equiv \mathbf{B} - \mathbf{B}_0$, subtracting any large-scale (mean) fields $\mathbf{V}_0$ and $\mathbf{B}_0$, and ρ is the mass density. If there is a mean magnetic field $\mathbf{B}_0$, then fluctuations in either pure $\pm$ state propagate along $\mp\mathbf{B}_0$ at the Alfvén speed, relative to the mean flow speed. Broadband turbulence as found in the solar wind (Coleman 1968) can also approximately satisfy this relation, in which case it is commonly termed Alfvénic turbulence. Of course, a superposition of both states in Eq. (1) is required in incompressible MHD, to support active nonlinear interactions, in which case pure propagation properties are no longer present (Moffatt 1978). Turning to the compressible case, such large-amplitude fluctuations in a pure + or − polarization state can satisfy the MHD equations provided that the total magnitude of the field, $|\mathbf{B}| = |\mathbf{B_0} + \mathbf{b}|$, is uniform (Goldstein et al. 1974; Barnes & Hollweg 1974; Barnes 1979). Such states are sometimes called states of spherical polarization (Barnes 1981). In the solar wind, Alfvénic fluctuations predominantly have the sign appropriate for outward propagation relative to the solar wind plasma.

Physically, local uniformity of $|\mathbf{B}|$ represents balance of the magnetic pressure $B^2/(2\mu_0)$. One might expect approximate magnetic pressure balance to be more likely when the magnetic pressure dominates over other types of pressure, e.g., when the plasma β (ratio of plasma pressure to magnetic pressure) is much less than unity. Indeed, Klein et al. (1993) found that at times of relatively low plasma β and high solar wind speed, the minimum variance directions of magnetic and velocity fluctuations from *Helios* data were better aligned with the mean magnetic field. Similar results were found by Smith et al. (2006) in *ACE* data at 1 AU and by Pine et al. (2020) in *Voyager* 1 and 2 data for r from about 1 to 32 au; that is, in low β plasma, fluctuations are more anisotropic and transverse to the mean field, which of course promotes more constant $|\mathbf{B}|$.

In turbulence, approximate magnetic pressure balance may result from rapid, local relaxation processes that also favor patches of flow-field alignment (Servidio et al. 2008). It has also been attributed to conservation of ion kinetic energy in the reference frame of observed alpha particle motion (Matteini et al. 2015). In any case, the divergence requirement on the magnetic field limits the spatial region over which $|\mathbf{B}|$ can remain uniform (Barnes 1979).

In situ measurements by various space missions, especially the *Helios* missions that collected data as close as 0.29 au from the Sun during 1974-1984, indicated that the solar wind is more Alfvénic while closer to the Sun (Bruno et al. 2007). The *Parker Solar Probe (PSP)* spacecraft, launched in 2018 August, approached within 0.17 au of the Sun during its first three solar encounters (hereafter referred to as E1-E3) and within 0.13 au during its fourth and fifth solar encounters (E4 and E5). *PSP* data have revealed even stronger Alfvénicity at lower radius (D'Amicis et al. 2021; Telloni et al. 2021), with increasing dominance of outward-propagating compared with inward-propagating Alfvénic fluctuations (Chen et al. 2020). Note that Alfvénicity can be defined in terms of various characteristics; in addition to near uniformity of $|\mathbf{B}|$, it can be measured in terms of the cross-helicity, Alfvén ratio, residual energy, and alignment angle between $\mathbf{b}$ and $\mathbf{v}$ (Parashar et al. 2020). There has also been much excitement over *PSP* observations of large-amplitude $\mathbf{b}$ and $\mathbf{v}$ fluctuations, and in particular fluctuations that change the orientation of $\mathbf{B}$ to the extent that the measured radial component B_R temporarily reverses and the magnetic field lines make S-shaped bends known as "switchbacks" (e.g., Kasper et al. 2019; Bale et al. 2019; Dudok de Wit et al. 2020; Mozer et al. 2020), which has given rise to a variety of explanations (e.g., Squire et al. 2020; Fisk & Kasper 2020; Ruffolo et al. 2020; Zank et al. 2020; Schwadron & McComas 2021; Drake et al. 2021).

Previous work has remarked upon domains of nearly constant $|\mathbf{B}|$ punctuated by sharp changes in *PSP* data (Ruffolo et al. 2020). They interpreted the domains of Alfvénic turbulence with nearly constant $|\mathbf{B}|$ as (possibly merged) mixing layers, which exhibit sharp boundaries as topological defects across which the dynamics have not yet balanced the magnetic pressure. Close to the Alfvén critical zone, where the solar wind speed begins to exceed the Alfvén speed, such mixing layers, including enhanced fluctuations and switchbacks, should have a spatial distribution that is closely related to the underlying streamer/flux-tube structure of the solar corona, with angular scales related to supergranulation. The domain boundaries typically involve major changes in the components of $\mathbf{B}$, often but not always including switchbacks. These boundaries may also correspond to sharp jumps in the magnetic field vector as indicated by a high partial variance of increments (PVI; Greco et al. 2008), and the waiting time distribution be-

tween high PVI events in *PSP* data has been analyzed by Chhiber et al. (2020).

In the present work we examine such domains of approximate magnetic pressure balance in more detail, starting with a prescription for identifying domains from time series of magnetic field measurements. We then analyze the distribution of domain duration T_D and in particular the mean domain duration as a function of time t and heliocentric distance r in comparison with plasma parameters such as plasma β. We also investigate the filling fraction of domains as a measure of Alfvénicity, and test simple frozen-in models of their aspect ratio by comparing the mean domain duration with the solar wind velocity relative to the spacecraft.

2. IDENTIFICATION OF DOMAINS

2.1. *Observational Data*

We proceed by analyzing publicly available data from the first five orbits (E1-E5) of *Parker Solar Probe*, from two instrument suites, FIELDS (Bale et al. 2016) and SWEAP (Kasper et al. 2016).[1] We used Level 2 magnetic field data from FIELDS, which typically have a data rate of 299 Hz, and Level 3 plasma data from SWEAP's Faraday cup component (SPC), typically available at a cadence of 0.87 s. We then resampled the data to 1-s cadence. Components of vector fields are expressed in the standard spacecraft-centered orthogonal RTN coordinate system, where +R is radial (antisunward), +T is tangential (toward increasing heliolongitude), and +N is normal (toward increasing heliolatitude).

We used magnetic field data to identify domains of nearly constant $|\mathbf{B}|$, both magnetic field and plasma data to calculate plasma β, and plasma velocity data to examine the aspect ratio of the domains. To compare the mean domain duration with $\log\beta$ over 1-d time intervals, we first calculated separate 1-h averages of B^2 and of n_pT_p, the proton number density times temperature, in the case that at least 10% of the 1-s data were available; otherwise the 1-h period was considered to have insufficient data. (Squaring or multiplication was performed before averaging in order to reduce fluctuations, e.g., as n and T are sometimes anticorrelated.) These average quantities were then combined using the approximation $\beta \approx 2\beta_p$ to estimate $\log\beta$ for each hour (including protons and their associated electrons but not the contributions of alpha particles and minor ions), and these were averaged to determine $\langle\log\beta\rangle$ for the 1-d time period. We should keep in mind that the plasma temperature from SPC measurements, which contributes to the calculation of plasma pressure and plasma β, is mainly derived from the measured distribution of V_R. If more than half of the 1-h periods had insufficient data, then that 1-d time period was considered to have insufficient data.

We made use of two data products from SWEAP/SPC for the solar wind velocity: 1) V_MOMENT_SC, the solar wind velocity relative to the *PSP* spacecraft, and 2) V_MOMENT, the solar wind velocity relative to an inertial frame, that is, the spacecraft velocity has been subtracted out of the solar wind velocity measurement.[2] We first used a time-domain Hampel filter (Davies & Gather 1993), with a filtering interval of 120 s and outliers identified as values more than three times larger than the local standard deviation. Also, we found that these two data products have some independent and spurious fluctuations. This provides a useful way to cross-check the data by subtracting the two velocity vectors to infer the spacecraft velocity, which must obey the laws of orbital mechanics. From this we determined estimates of the spacecraft orbital energy and angular momentum, which should remain nearly constant (except at times of Venus encounters, which changed *PSP*'s orbit). We first rejected 1-s data values for which these quantities deviated greatly (by $\gtrsim$50%) and performed 1-h averages in the case that at least 10% of the 1-s data were available; otherwise the 1-h period was considered to have insufficient data. Then we examined the distributions of the 1-h averages of these quantities, fit the peak regions by a Gaussian function, and rejected 1-h time periods that deviated from the mean by more than three standard deviations. When computing a 1-d moving average, if more than half of the 1-h periods therein were missing or rejected, then that 1-d time period was considered to have insufficient velocity data.

2.2. *Definition and Selection of Domains*

Domains of Alfvénic fluctuations were conceptually introduced by Ruffolo et al. (2020). Here, we have developed a definition of contiguous domains of nearly constant magnetic field magnitude $|\mathbf{B}|$, which can be physically considered as domains of approximate magnetic pressure balance, or Alfvénic domains. Note that not all times are assigned to a domain. Defining domains as contiguous is somewhat different from the concept of Ruffolo et al. (2020), as we will discuss in Section 4.

Here domains are selected in two stages:

[1] All data were downloaded from https://cdaweb.gsfc.nasa.gov/pub/data/psp/

[2] See the SWEAP Data User's Guide.

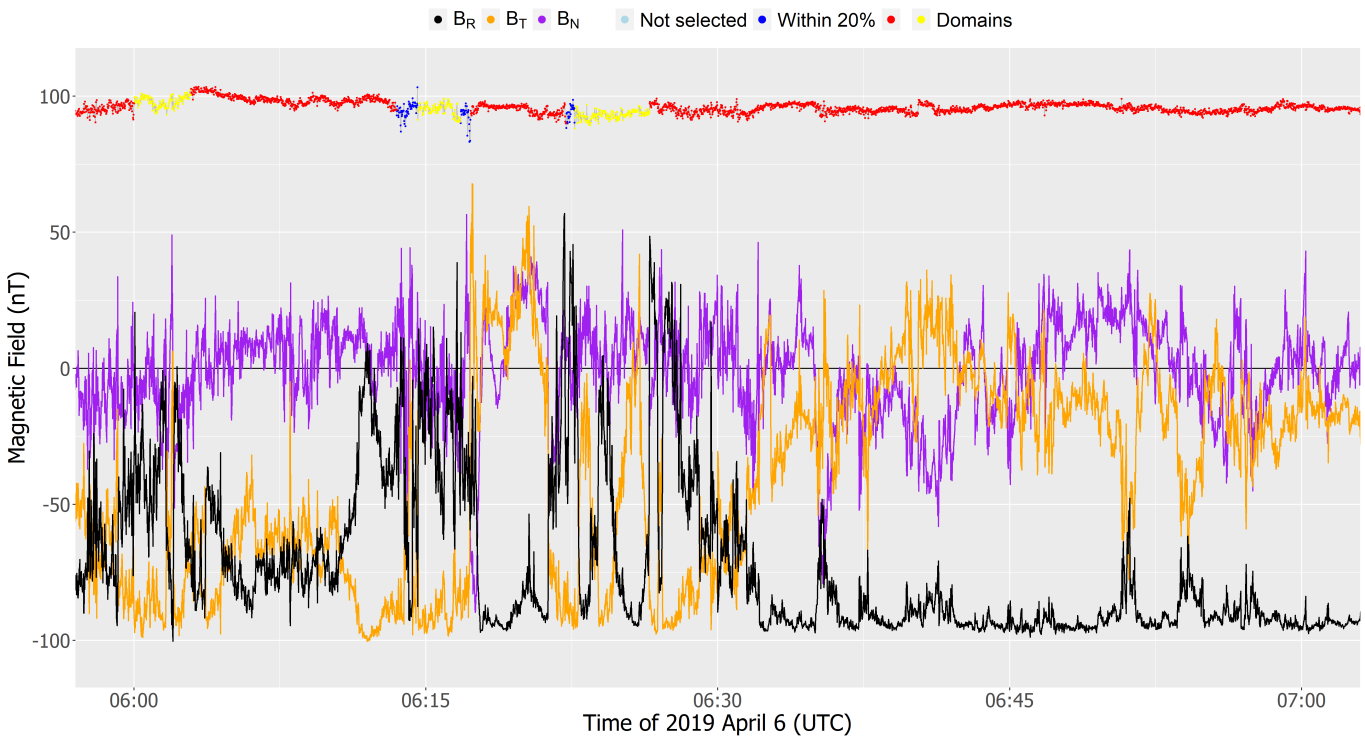

Figure 1. Magnetic field magnitude $|\mathbf{B}|$, with coloring to indicate selected domains of approximate magnetic pressure balance, and components B_R (black), B_T (orange), and B_N (purple) from 1-s sampling of *PSP*/FIELDS measurements during one hour (2019 April 6, 06.00-07.00 UTC), 32 h after the second *PSP* perihelion. Along the top trace, showing values of $|\mathbf{B}|$, light blue points are at times that were not selected in the first stage of domain selection, dark blue is for time periods with $|\mathbf{B}|$ constant within 20% but rejected in the second stage of domain selection, and alternating red and yellow coloring indicates selected domains. Domains are interrupted by particularly strong fluctuations in $\mathbf{B}$, some but not all of which involve reversals in the sign of B_R, i.e., switchbacks.

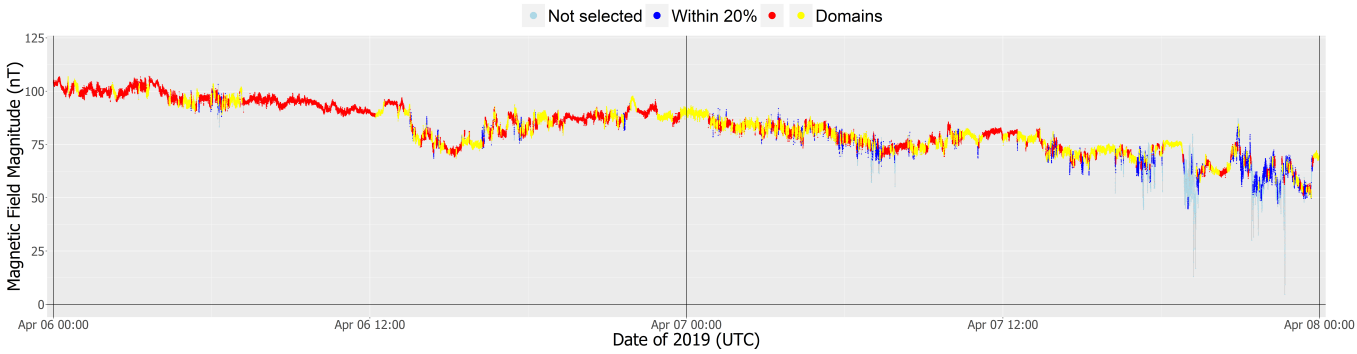

Figure 2. Magnetic field magnitude $|\mathbf{B}|$ and domains of approximate magnetic pressure balance identified from 1-s sampling of *PSP*/FIELDS measurements during 2019 April 6-7, a time period from 25 to 73 hours after the second *PSP* perihelion. Coloring as in Figure 1. The mean domain duration was much longer on April 6, in association with lower plasma β on that day.

1. Throughout the domain, the difference between the maximum and minimum magnetic field magnitude, $|\mathbf{B}|_{\rm max} - |\mathbf{B}|_{\rm min}$, should remain within a first-stage fractional tolerance of the minimum value ($f_1|\mathbf{B}|_{\rm min}$).

2. During each 600-s time period within the domain (or if the domain is shorter than 600 s, then over the entire domain), $|\mathbf{B}|_{\rm max} - |\mathbf{B}|_{\rm min}$ should remain within a second-stage fractional tolerance of the minimum value ($f_2|\mathbf{B}|_{\rm min}$).

We further require that domains have a duration of at least 60 s, in order to limit the number of very small domains. We tried changing this minimum duration, and found that the effect on the mean domain duration was

roughly uniform in time and did not significantly affect trends in our analysis. Therefore, we use 60 s as a time that is significantly shorter than the turbulent correlation time (see Parashar et al. 2020; Chen et al. 2020) while much longer than the 1-s cadence of our dataset. We also limit domains to contiguous time periods with no missing data.

The purpose for using two stages is to require the entire domain to remain within a fractional tolerance f_1 and to require variations within that tolerance to be relatively gradual, within a smaller fractional tolerance f_2 over 600 s, a value chosen to be of the order of the correlation time of the turbulence. In other words, turbulent fluctuations are allowed to vary within f_2 while longer-time variations are allowed within a larger tolerance f_1. We chose to specify these tolerances with a 2:1 ratio, so that $f_1 = 2f_2$.

To choose the tolerance values, we compared the results of domain selection for PSP data with different tolerances ranging from $f_2 = 0.02$ to 0.14. We monitored the filling fraction, i.e., the fraction of 1-s data that are assigned to a domain, with the view that a useful definition of domains should assign some but not all times to Alfvénic domains. Throughout the first 5 *PSP* orbits, we found that a high tolerance frequently yields a saturated filling fraction (FF=1) at low radius and a low tolerance frequently gives zero filling fraction at high radius. The intermediate values $f_2 = 0.08$ and 0.1 yield a filling fraction that usefully exhibits time variations (without saturation) at both low and high radius within the *PSP* orbits. Among these two values, $f_2 = 0.1$ (which implies $f_1 = 0.2$) provides a clearer relation between the mean domain duration and plasma β, so we adopt these as useful tolerance values. In summary, we define domains as contiguous time periods (of at least 60 s) when $|\mathbf{B}|$ remains constant to within 20% over the entire domain (first stage of selection) and within 10% over all 600-s time periods within the domain (second stage of selection).

As a check that the selection algorithm was implemented correctly, different members of our team developed separate computer programs to analyze the same data sets and obtained identical results, both for the numbers of domains and their durations.

2.3. *Examples and Properties of Domains*

Figures 1 and 2 show examples of the results of domain selection using the above prescription. Figure 1 includes data of magnetic field components and the magnitude $|\mathbf{B}|$ for one hour (2019 April 6, 06:00-07:00 UTC), 32 hours after the second *PSP* perihelion, while Figure 2 indicates domains selected during a two-day time period, 2019 April 6-7, which encompasses times from 25 to 73 hours after E2 perihelion. Along the trace for $|\mathbf{B}|$, we use coloring to indicate the results of our domain identification. Light blue points indicate 1-s data that were not selected even at the first stage. (Note that for the time period shown in Figure 1, all data were selected at this stage.) Dark blue indicates data that were selected in the first stage, i.e., were part of a time period during which $|\mathbf{B}|$ was constant within 20%, but were not selected in the second stage. Finally, the time periods selected as domains are indicated by alternating red and yellow coloring. Red and yellow colors have the same meaning, and are alternated to assist in distinguishing the boundaries of domains.

From Figures 1 and 2, one may observe that some time periods of up to several hours appear to have nearly constant $|\mathbf{B}|$, yet have alternating coloring, indicating that our algorithm selects multiple separate domains. In such cases, the key role of the algorithm is to identify interruptions of domains due to excessively rapid variation of the magnetic field magnitude. In some cases the interruption is an inclusion of different $|\mathbf{B}|$ between similar values before and afterward; in some other cases it represents a step from one level of $|\mathbf{B}|$ to another. Our present analysis does not distinguish between these possibilities, and in this sense may deviate from the conception of domains by Ruffolo et al. (2020), who considered a domain boundary to involve a step from one level of $|\mathbf{B}|$ to another.

In Figure 1, we often see large fluctuations of magnetic field components within a domain of nearly constant $|\mathbf{B}|$. These are likely examples of large-scale Alfvénic fluctuations. Such fluctuations within a domain can have large amplitudes in any of the components, including the radial component B_R. During this time period, B_R was most commonly near $-|\mathbf{B}| \approx -100$ nT, while fluctuations are termed "switchbacks" if they are sufficiently extreme that B_R reverses sign. In our view, switchbacks that occur within an Alfvénic domain are one type of large-amplitude Alfvénic fluctuation out of a continuum of possible amplitudes and directions (see also Dudok de Wit et al. 2020, who discuss a continuum of angular deflections of $\mathbf{B}$, not only whether a deflection exceeds 90° so that B_R reverses sign).

Figure 1 also shows various examples of domain boundaries, where domains are interrupted. These usually involve particularly strong fluctuations of magnetic field components, many but not all of which are switchbacks. For example, the first transition from a "yellow" to "red" domain, from 06:02:54 to 06:02:55 UTC, was not associated with a switchback (i.e., B_R did not reverse sign). Thus domain boundaries and switchbacks

are related, but not quite the same set of events: there are switchbacks that do not interrupt domains, and domain boundaries that do not include switchbacks.

Finally, we note that in Figure 2, which shows domains over 2019 April 6-7, the early part of April 6 clearly has a few domains of very long duration (up to several hours), while April 7 generally has much shorter domains. Such time variations in the mean domain duration and distribution of domain durations, as well as their filling fraction, are the subject of further analysis in this work.

3. CHARACTERIZATION OF DOMAINS

We proceed to characterize domains of approximate magnetic pressure balance in data from the first five orbits of *PSP*. We first examine variations in the mean domain duration. Average duration varies strongly with plasma β, with longer average duration associated with lower β. We then examine distributions of domain duration for high or low ranges of plasma β, which can be characterized by broken power laws. Next, we consider the aspect ratio of the domains, in the context of a frozen-in approximation. We also report the filling fraction of domains, which is strongly variable but overall has a decreasing trend with increasing distance from the Sun.

3.1. *Relationship of Domain Duration with Plasma β*

Now let us consider the variation of the mean domain duration and its dependence on plasma β. Given that individual domains can last for up to several hours (see Figure 2), we choose to average over 1-d time periods. To reduce the sensitivity to the day boundary, and to provide some information about time variation over scales less than one day, we determine the mean domain duration and other quantities over running 1-d averages computed with a 6-h cadence.

Such averages of the mean domain duration and related quantities are shown as a function of time (centroid of the averaging interval) in Figures 3-7 for the first five *PSP* orbits, E1-E5, respectively. For each of these figures, panel (a) shows the mean domain duration, $\langle T_D \rangle$. Panel (b) shows the plasma β, derived from *PSP* data as described in Section 2.1. Panels (c)-(e) show measures of the solar wind velocity relative to the spacecraft, which will be discussed in Section 3.3 in connection with the aspect ratio of domains. Note that for Figures 3-7, panels (a)-(e) all use logarithmic vertical scales with the same spacing per decade to facilitate quantitative comparison. Panel (f) shows the filling fraction, and (g) plots the radial distance from the Sun.

Figures 3 and 4 show a clear inverse association between the mean domain duration and plasma β during E1 and E2. During these orbits, the 1-d-averaged

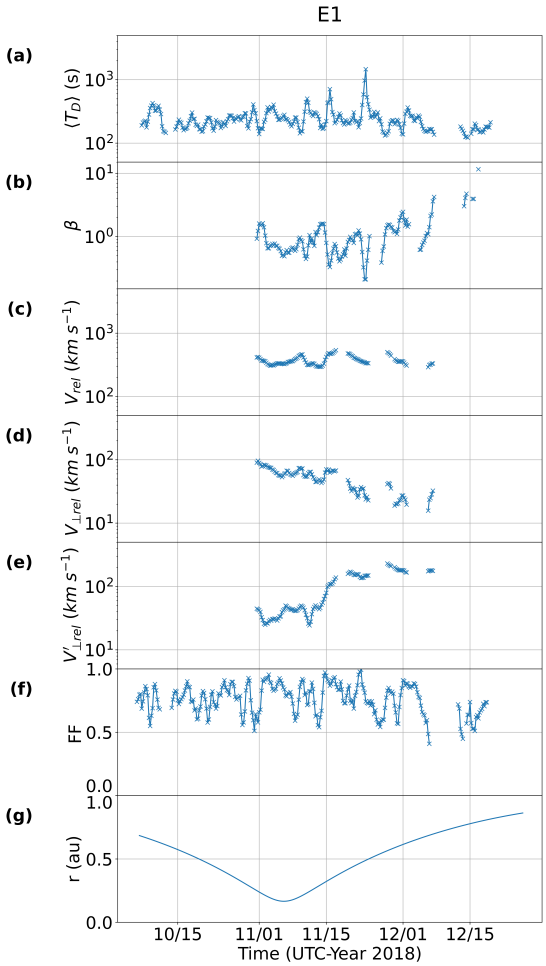

Figure 3. Time series during the first *PSP* orbit. Mean values of (a) domain duration, T_D; (b) plasma β; (c) magnitude of the solar wind velocity relative to the spacecraft, V_{rel}; (d) magnitude of the solar wind velocity relative to the spacecraft and perpendicular to the radial direction, $V_{\perp rel}$; (e) magnitude of the solar wind velocity relative to the spacecraft and perpendicular to the Parker spiral direction, $V'_{\perp rel}$; (f) filling fraction, FF; (g) radius from the Sun, r. Panels (a)-(f) show running 1-d averages with 6-h cadence, plotted at the centroid of the averaging interval. The largest values of mean domain duration $\langle T_D \rangle$ are associated with periods of low plasma β. Results for $\langle T_D \rangle$ are inconsistent with inverse proportionality to $V_{\perp rel}$ or $V'_{\perp rel}$, as would be expected if domains were elongated structures along the radial or Parker spiral direction, respectively.

plasma β varied over $\sim$1.5 orders of magnitude. During E3 (Figure 5), the relevant plasma data were available for relatively few time periods, which mostly exhibited weaker variations in β, making it difficult to identify a clear trend (see Figure 5). Figure 8(a) combines data from these first three orbits, each of which reached a perihelion distance of 0.17 au, to demonstrate that $\langle T_D \rangle$ generally decreases with increasing plasma β. For com-

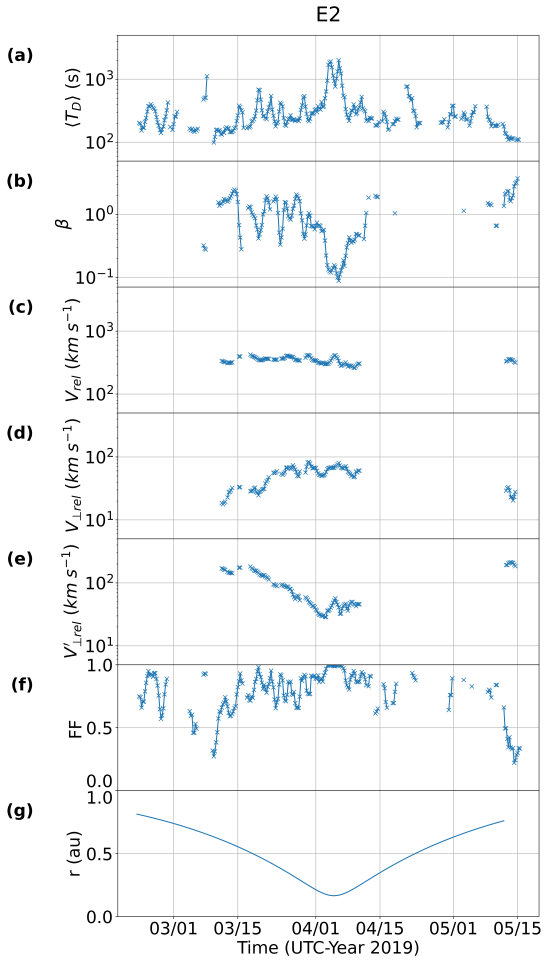

Figure 4. Time series during the second *PSP* orbit, as in Figure 3. The largest values of mean domain duration $\langle T_D \rangle$ are associated with periods of low plasma β. Results for $\langle T_D \rangle$ are inconsistent with inverse proportionality to $V_{\perp rel}$, as would be expected if domains were elongated structures along the radial direction.

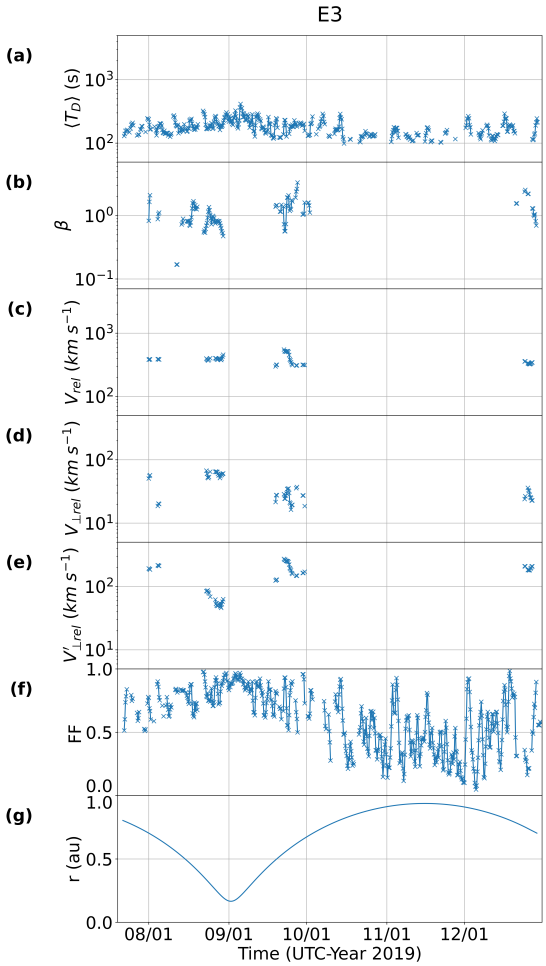

Figure 5. Time series during the third *PSP* orbit, as in Figure 3. Results for $\langle T_D \rangle$ are inconsistent with inverse proportionality to $V_{\perp rel}$ or $V'_{\perp rel}$, as would be expected if domains were elongated structures along the radial or Parker spiral direction, respectively. The filling fraction, FF, has a strong inverse relation with the radius, r.

parison, the dashed line shows a trend of inverse proportionality, $\langle T_D \rangle \propto \beta^{-1}$, though with considerable scatter in the data relative to that trend.

Near E2 perihelion, there was an interesting time period with 1-d-averaged β of ∼0.1 and the largest mean domain durations found in all of the first five orbits (see also Figures 1 and 2). This time period was examined in detail by Rouillard et al. (2020), including a comparison of *PSP* data with white-light coronagraph images from the LASCO instrument suite on the *Solar and Heliospheric Observatory* (*SOHO*) mission and other instruments. They found that near E2 perihelion, *PSP* was usually inside streamers with high normalized density nr^2, but for two time periods on 2019 April 3-6 and April 6-7, *PSP* exited these streamers and entered regions of lower normalized density. These correspond to the times of very low β and highest mean domain duration in our analysis.

For encounters E4 and E5, plasma β data again exhibit strong variations with time, as illustrated in Figures 6 and 7. The mean domain duration generally exhibits an inverse association with β. There are some notable exceptions to this, including some time periods near or shortly before E4 and E5 perihelia, when β had very low values while $\langle T_D \rangle$ was only moderately high. Figure 8(b) combines data for $\langle T_D \rangle$ as a function of β for E4 and E5, when *PSP* reached a perihelion at 0.13 au. For the E4 and E5 orbits, there is still an overall inverse relationship, though it is not as dramatic as for E1-E3.

Low β indicates a dominance of magnetic pressure over plasma pressure, a condition that may favor main-

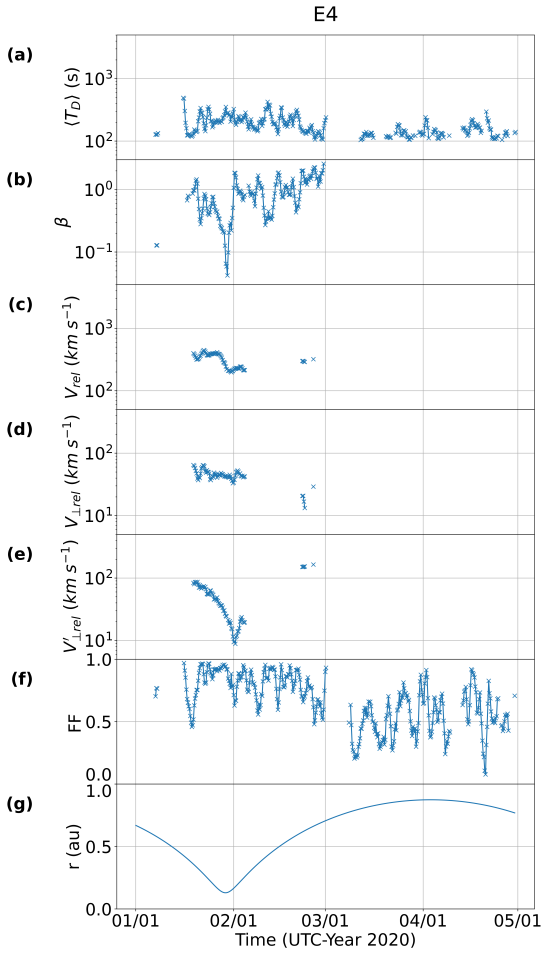

Figure 6. Time series during the fourth *PSP* orbit, as in Figure 3. Results for $\langle T_D \rangle$ are inconsistent with inverse proportionality to $V_{\perp rel}$ or $V'_{\perp rel}$, as would be expected if domains were elongated structures along the radial or Parker spiral direction, respectively. The filling fraction, FF, has an inverse relation with the radius, r.

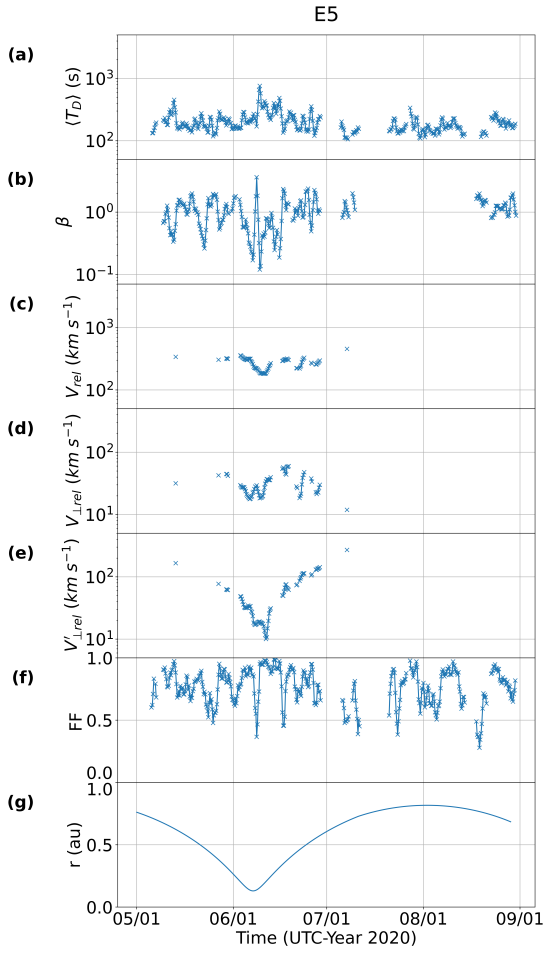

Figure 7. Time series during the fifth *PSP* orbit, as in Figure 3. Results for $\langle T_D \rangle$ are inconsistent with inverse proportionality to $V'_{\perp rel}$, as would be expected if domains were elongated structures along the Parker spiral direction.

tenance of good pressure balance over longer time periods. Therefore, it is physically reasonable that low β is associated with longer mean domain duration $\langle T_D \rangle$. The results in Figure 8 show a continuous and extended relationship, in which increasing β is associated with decreasing $\langle T_D \rangle$, even for relatively high $\beta > 1$. As mentioned in the introduction, previous work also found that at times of relatively low plasma β, the minimum variance directions of magnetic and velocity fluctuations were better aligned with the mean magnetic field, consistent with relative constancy of $|\mathbf{B}|$ (Klein et al. 1993; Smith et al. 2006; Pine et al. 2020). We address this issue further in the discussion section.

Figure 9 displays the mean domain duration $\langle T_D \rangle$ and plasma β as a function of *PSP*'s location along its orbit for E1, E2, E4, and E5. Note that these represent views from ecliptic North, in which *PSP* orbits counterclockwise around the Sun (yellow circle at $x = 0$, $y = 0$). We do not show a plot for E3 because of the relative paucity of plasma data. The circle size indicates the domain duration, and the color scale indicates $\log(\beta)$. During most orbits, β was lowest near each encounter's perihelion, though this was not the case for E1, during which β was lowest over two weeks after the perihelion.

Figures 3-7 and Figure 9 indicate no apparent relationship between the mean domain duration $\langle T_D \rangle$ and distance r from the Sun, except insofar as $\langle T_D \rangle$ depends on plasma β.

3.2. *Domain Duration Distribution*

Because plasma β has a strong effect on the mean domain duration, as seen above, we have also examined its effect on the distribution of the domain duration T_D. Such distributions are shown in Figure 10 for times of relatively low or high plasma β during the second orbit, E2. Specifically, the low β range is for $\log(\beta) < -0.8$

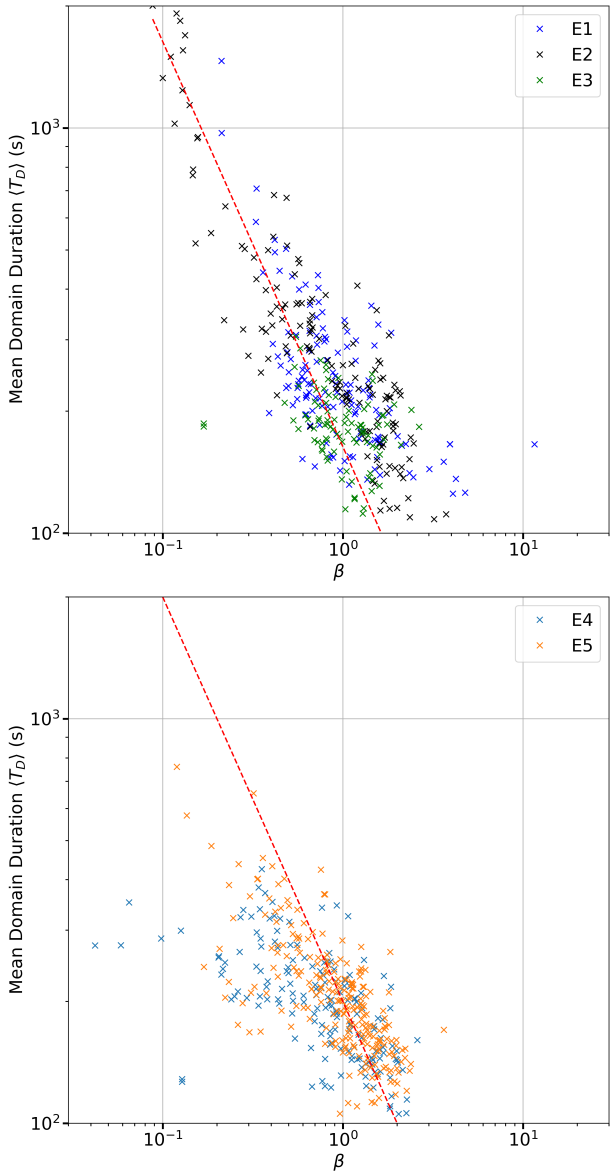

Figure 8. Mean domain duration $\langle T_D \rangle$ as a function of plasma β for (a) E1-E3 and (b) E4-E5. Each data point represents a running 1-d average with 6-h cadence. There is a general trend of decreasing $\langle T_D \rangle$ with increasing β. Dashed line represents $\langle T_D \rangle \propto \beta^{-1}$.

($\beta < 0.16$, red symbols). In this case, $\beta \ll 1$ and the magnetic pressure is dominant over plasma pressure. The relatively high β range is for $\log(\beta) > -0.25$ ($\beta > 0.56$, blue symbols), which for this data set corresponds to $\beta \sim 1$ (see Figure 4), with roughly equipartitioned magnetic and plasma pressure. These distributions were computed by acquiring counts in bins of T_D values, each bin having equal width on a log scale. We then plot the distribution function dN/dT_D, defined as the number of domains in each bin divided by the T_D bin width. In this way the distributions are normalized to the number of cases. Therefore, for higher β, the distributions have greater dN/dT_D simply because there were more instances of higher β in the data set.

We find the distributions to have a broken power-law form, with a break at $T_{D,b} \approx 500$ s, which is on the order of the correlation time (noting that the correlation time varies significantly over the initial *PSP* orbits; Chen et al. 2020). We have performed separate power-law fits, $dN/dT_D \propto T_D^{\alpha}$, to each distribution for $T_D \ll T_{D,b}$ and $T_D \gg T_{D,b}$. For the lower β range we find power-law indices $\alpha = -0.75 \pm 0.22$ for low T_D and $\alpha = -1.64 \pm 0.21$ for high T_D. For the higher β range we find power-law indices $\alpha = -1.70 \pm 0.03$ for low T_D and $\alpha = -2.33 \pm 0.08$ for high T_D.

In the previous subsection, we reported that times of lower β generally have higher values of $\langle T_D \rangle$, which is physically reasonable because they have stiffer magnetic resistance to disturbance of magnetic pressure balance. Figure 10 and the power-law indices demonstrate that at lower plasma β, not only is the mean duration greater, but the entire distribution is quite different, with higher values of the power-law indices and a relative enhancement of longer domain durations. We will discuss the possible physical significance of the broken power-law distributions in Section 4.

3.3. *Aspect Ratio*

We now consider hypotheses that our data for the mean domain duration $\langle T_D \rangle$ can be described by spatial structures of various aspect ratios that convect past the spacecraft along with the solar wind. Such convection would imply that $\langle T_D \rangle$ is inversely proportional to a measure of the relative velocity between the solar wind and the spacecraft, so we can use such a relation to test each hypothesis. Because plasma β has a strong influence on $\langle T_D \rangle$, we compare $\langle T_D \rangle$ with a measure of relative velocity using time periods that have similar β values.

First, consider the hypothesis in which domains are spherical or isotropic with a constant size distribution that does not depend on time or distance from the Sun. The time duration over which PSP crosses a sphere should relate to the relative speed between the solar wind and the spacecraft, i.e., $V_{rel} = |\mathbf{V} - \mathbf{V}_s|$, where $\mathbf{V}$ is the solar wind velocity and $\mathbf{V}_s$ is the velocity of the spacecraft. More precisely, for a sphere of radius a, a random transept through the sphere has a mean length of $(4/3)a$. Accordingly we expect the mean duration of transit through the sphere to be

$$\langle T_s \rangle = \frac{4}{3} \frac{a}{V_{rel}}, \tag{2}$$

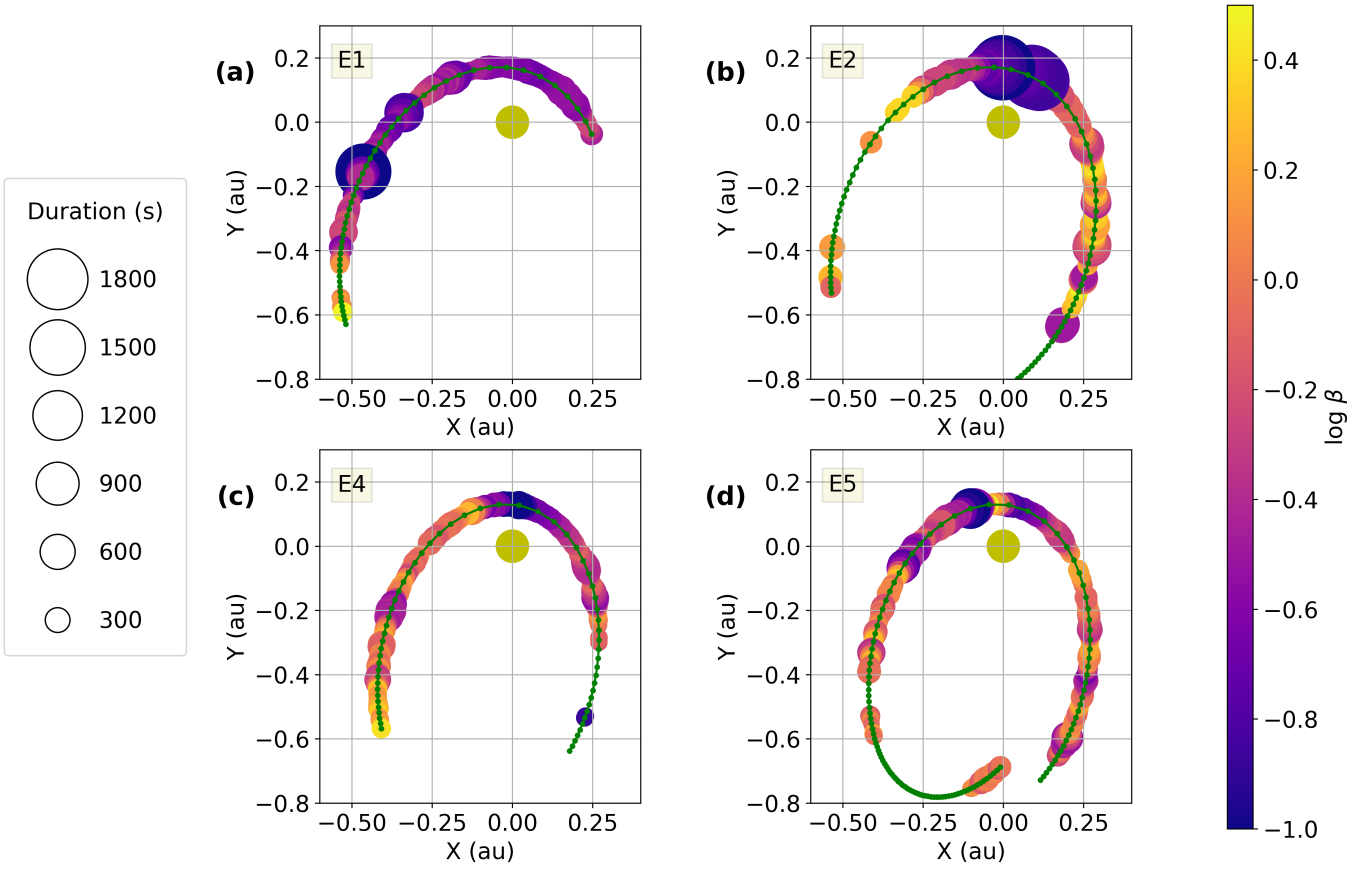

Figure 9. Mean duration of domains of approximate magnetic pressure balance $\langle T_D \rangle$ (indicated by circle size) and plasma β (indicated by color scale) as a function of the location of *PSP* as it orbited counterclockwise around the Sun (yellow circle at $x = 0$, $y = 0$), for orbits E1, E2, E4, and E5. Small green markers represent the location of *PSP* at the start of each day. Data of $\langle T_D \rangle$ and β are shown for 1-d averages with 6-h cadence. It is seen that $\langle T_D \rangle$ generally has an inverse relationship with β and is otherwise not dependent on distance from the Sun.

where

$$V_{rel} \equiv \sqrt{(V_R - V_{s,R})^2 + (V_T - V_{s,T})^2 + (V_N - V_{s,N})^2}, \quad (3)$$

and we have expressed $V_{rel} = |\mathbf{V} - \mathbf{V}_s|$ in terms of the velocity components. More generally, for a uniform and constant distribution of the size a, we can expect that $\langle T_D \rangle \propto 1/V_{rel}$.

If domains are delineated by strong magnetic fluctuations that interrupt the near constancy of $|\mathbf{B}|$, these need not form a continuous boundary around the domain, and the actual duration of domains would depend on how frequently the spacecraft trajectory encounters such interruptions. Thus the hypothesis for isotropic domains, and $\langle T_D \rangle \propto 1/V_{rel}$, would apply to a case where strong fluctuations that interrupt domains have a uniformly random distribution in space, or are otherwise distributed such that a trajectory along any orientation encounters such interruptions with the same spatial distribution.

Next, suppose that domains are shaped as tubes that are highly elongated along the R (radial) direction, with circular dimension b in the T and N directions. This hypothesis is motivated by the work of Horbury et al. (2020), who found that Alfvénic "spikes," including switchbacks, observed in *PSP* data have a large aspect ratio, shaped as long, thin structures oriented roughly along the radial direction. In this case, entering and exiting the domain is determined only in the T and N directions, so we consider the relative velocity between the solar wind and the spacecraft in only these directions, i.e., perpendicular to the radial direction. A random transept in two dimensions through the circular cross-section has mean length $(\pi/2)b$. Thus the mean time to cross the tube is

$$\langle T_t \rangle = \frac{\pi}{2} \frac{b}{V_{\perp rel}} \quad (4)$$

where

$$V_{\perp rel} \equiv \sqrt{(V_T - V_{s,T})^2 + (V_N - V_{s,N})^2}. \quad (5)$$

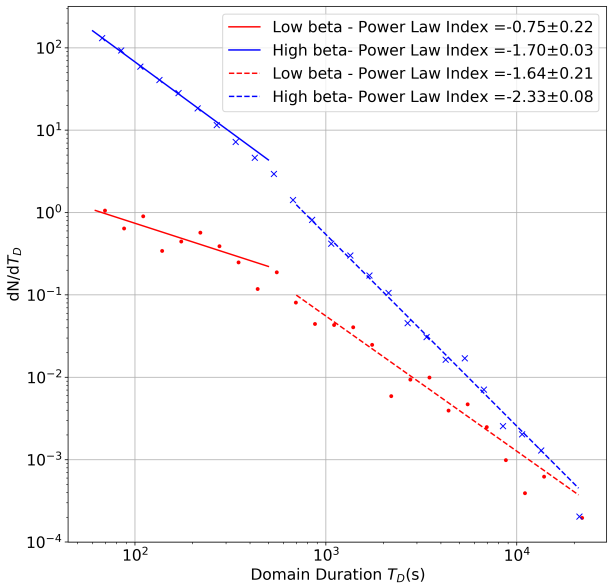

Figure 10. Distributions of domain duration T_D during E2, for times of $\beta < 0.16$ (red symbols) and $\beta > 0.56$ (blue symbols). The distributions have a broken power-law form with a break on the order of the correlation time. The lower β range has stiffer magnetic resistance to disturbance of magnetic pressure balance, leading to a distribution weighted toward higher T_D values.

For a distribution of the size b that is uniform and constant in space, this hypothesis implies that $\langle T_D \rangle \propto 1/V_{\perp rel}$. This hypothesis also includes the case in which domains are interrupted by strong magnetic fluctuations, if those are arranged in a roughly two-dimensional pattern with a spacing in the T and N directions that is statistically homogeneous, constant, and axisymmetric. A pattern of radially aligned magnetic flux tubes, each with a distinct value of $|\mathbf{B}|$, is also included in this case.

Finally, we consider a third hypothesis, similar to the second but in which domains represent structures elongated along the local Parker spiral direction, i.e., the expected direction of the large-scale interplanetary magnetic field based on the measured local solar wind speed and the rate of solar rotation (Parker 1958). This hypothesis is inspired by the work of Laker et al. (2021), who inferred that switchbacks in *PSP* data are long, thin structures oriented along the Parker spiral direction. For this hypothesis, we expect that $\langle T_D \rangle \propto 1/V'_{\perp rel}$, where $V'_{\perp rel}$ is the magnitude of the projection onto a plane perpendicular to the local Parker spiral direction of the solar wind velocity relative to the spacecraft.

Therefore, we consider three measures of the relative velocity, V_{rel}, $V_{\perp rel}$, and $V'_{\perp rel}$, as relevant for examining these three hypotheses for extreme cases of the aspect ratio of domains. In Figures 3-8, these three measures are plotted in panels (c)-(e), respectively. We then compare the time series of $\langle T_D \rangle$ (panel (a)) with those in panels (c)-(e), keeping in mind that each hypothesis implies an inverse proportionality between $\langle T_D \rangle$ and the relevant measure of the relative velocity, for times of similar plasma β. Note that panels (a)-(e) are all plotted with the same logarithmic scale size to assist in the comparison.

For each of the first five orbits, V_{rel} (panel (c)) exhibits only moderate variation, so the data do not rule out the relationship $\langle T_D \rangle \propto V_{rel}^{-1}$, as expected for spherical or isotropic domains, nor do they provide supporting evidence for such a relationship.

In contrast, for E1-E4 (Figures 3-6), the time series for $\langle T_D \rangle$ (panel (a)) and $V_{\perp rel}$ (panel (d)) are inconsistent with an inverse proportionality $\langle T_D \rangle \propto V_{\perp rel}^{-1}$. Similarly, for E1 (Figure 3) and E3-E5 (Figures 5-7), the time series in panel (a) and for $V'_{\perp rel}$ (panel (e)) are inconsistent with an inverse proportionality $\langle T_D \rangle \propto (V'_{\perp rel})^{-1}$. Therefore, our results are inconsistent with domains delineated by very elongated shapes along the radial or local Parker spiral direction that convect past the spacecraft with the solar wind.

3.4. *Filling Fraction*

We use the term "filling fraction" (FF) to refer to the fraction of 1-s data points that are assigned to any domain, using the definition and procedure adopted in Section 2.2. The time series of FF for E1-E5 are plotted in panel (f) of Figures 3-7. Though FF exhibits strong variations, it is clear, especially for E3 and E4 (Figures 5-6), that FF is usually close to 1 near perihelion and can be significantly lower at greater distance r from the Sun (plotted in panel (g)). We have not found an association of FF with plasma β, crossing of the heliospheric current sheet, or other physical features of the solar wind, other than the distance from the Sun.

We have computed the median FF values from all five orbits for different ranges of r, and we found the very different median values of 0.90 for $0.1 < r < 0.2$ au and 0.38 for $0.9 \leq r < 1.0$ au. While a high FF indicates that most of the selected data points are assigned to domains, these could either be a large number of short domains or a smaller number of longer domains, as indicated by the mean domain duration. The filling fraction of a time range can be interpreted as a quantitative measure of its Alfvénicity, so our finding that FF varies strongly with r is consistent with numerous findings in the literature that the solar wind is more frequently Alfvénic at closer distances to the Sun (see Section 1).

4. DISCUSSION

Parker Solar Probe continues to explore the inner solar wind at previously unattained proximity to the Sun,

affording observers and theorists alike opportunities to examine distinctive features of the plasma and fields approaching the Alfvén critical region (DeForest et al. 2016; Kasper et al. 2019; Bale et al. 2019). Much attention has been given to switchbacks, jets and large-amplitude, high cross-helicity fluctuations observed in this region with vigorous ongoing debate concerning the origin and expected evolution of such structures (Squire et al. 2020; Fisk & Kasper 2020; Ruffolo et al. 2020; Zank et al. 2020; Schwadron & McComas 2021; Drake et al. 2021). So far, considerable emphasis has been placed on quantifying Alfvénicity and magnetic field reversals (switchbacks), as well as details such as directionality of strahl and energetic particles, and general turbulence properties in the vicinity of these distinctive fluctuations. Here we have examined in some detail a related but distinct feature of the magnetic field near PSP perihelia that, as far as we are aware, has not as yet been studied and quantified in detail as a separate phenomenon: the organization of the magnetic field into local domains of near constant field magnitude.

The present work defines a domain of approximate magnetic pressure balance, or Alfvénic domain, as a contiguous set of data over which $|\mathbf{B}|$ varies within prescribed limits (see Section 2.2). This local definition allows examination of:

1. Well-defined, quantitative measures.

2. The mean duration, which relates to plasma β and the frequency of interruptions, which in turn relates to PVI events and switchbacks.

3. The filling fraction (because not all times are assigned to a domain), which serves as another measure of the Alfvénicity of an extended time period.

4. The aspect ratios of uninterrupted regions of nearly constant $|\mathbf{B}|$.

The domain duration defined in this work does not characterize the overall constancy of $|\mathbf{B}|$ over an extended time period, unless that time period is free of interruptions to near-constancy of $|\mathbf{B}|$. For example, consider Figures 3 and 4 of Telloni et al. (2021), who showed time series of the magnetic field components and magnitude for a parcel of solar wind as it passed *PSP* at $r \approx 0.1$ au (near E6 perihelion) and later passed the Solar Orbiter (SolO) spacecraft at $r \approx 1.0$ au. They commented that the solar wind plasma was more Alfvénic at 0.1 au, and from their figures the time series of $|\mathbf{B}|$ at 0.1 au was clearly much more constant (in fractional terms) than $|\mathbf{B}|$ at 1.0 au. Yet the present work finds that the mean domain duration generally does not depend on r, except insofar as it depends on plasma β. (Plasma β can evolve with distance from the Sun. Such evolution was not measured for the solar wind parcel studied by Telloni et al. (2021) because SolO plasma measurements were not available for the relevant time period.) The reason is that our domain analysis does not address the overall constancy of $|\mathbf{B}|$ over such extended time periods; instead, it relates to local magnetic pressure balance and turbulent relaxation. Indeed, from Figure 3 of Telloni et al. (2021), it is seen that when the parcel of solar wind was at 0.1 au, there were numerous interruptions to near constancy of $|\mathbf{B}|$. Such interruptions or domain boundaries may be interpreted as fault lines across which the solar wind plasma can evolve independently and thereafter have different values of $|\mathbf{B}|$ in different domains. We further note that our filling fraction of domains does provide a measure of Alfvénicity of extended time periods, and this indeed does exhibit a strong dependence on r.

Domains of nearly constant $|\mathbf{B}|$ were introduced by Ruffolo et al. (2020), although they were not clearly defined or systematically examined. That work noted an extended period of nearly constant $|\mathbf{B}|$ on 2018 Nov 11, 5 days after E1 perihelion, based on which they discussed the possibility that domain durations increase with increasing distance from the Sun. (Their Figure 11(c) shows a histogram, said to be for 0000-0800 UT, but upon closer examination their data set ended at about 0325 UT.) For this case, our domain analysis does find an uninterrupted domain for nearly 5 hours, and this was a time period of moderately low β. More generally we find that the mean domain duration has a strong inverse relation with β, but otherwise no apparent dependence on r.

Given that domain boundaries represent interruptions of near constancy of $|\mathbf{B}|$, they are often related to strong magnetic fluctuation events, such as switchbacks and magnetic PVI events. For the example shown in Figure 1, most of the domain boundaries involve switchbacks, while roughly half of the switchbacks or switchback patches disrupt a domain, i.e., involve a substantial change in $|\mathbf{B}|$. Therefore, our distributions of domain duration (see Figure 10), which have broken power-law forms, can be interpreted as waiting time distributions between such interruptions. Previous work has addressed the waiting-time distributions of *PSP* observations of switchbacks (Dudok de Wit et al. 2020) and magnetic PVI events (Chhiber et al. 2020). For both cases, the reported distributions exhibited a power-law form with a break at $\sim 10^2 - 10^3$ s, as in our results, roughly corresponding to the turbulence correlation time. Our results extend to durations over 10^4 s,

allowing us to identify another power-law for $T_D > T_{D,b}$, above the break duration. The switchback waiting time distributions of Dudok de Wit et al. (2020) are also consistent with broken power laws, while the PVI waiting time distributions of Chhiber et al. (2020) did not extend to such long times, making it difficult to unambiguously determine the distribution shape above the break time.

For short durations with $T_D < T_{D,b}$, below the turbulence correlation scale, i.e., in the inertial range of turbulence, it is unsurprising to obtain power-law distributions as these are characteristic of scale-invariant phenomena. For the power-law index at lower times, Dudok de Wit et al. (2020) obtained $\alpha = -1.4$ to -1.6, while Chhiber et al. (2020) obtained $\alpha = -0.6$ to -1.3. Our distributions for E2 yielded $\alpha = -0.75 \pm 0.22$ for $\beta < 0.16$ and $\alpha = -1.70 \pm 0.03$ for $\beta > 0.56$, which are reasonably consistent with the previous results. Chhiber et al. (2020) pointed out that for comparison, the waiting time distribution of the Cantor set, a classic example of a highly clustered set of events (Cantor 1883), is a power law with $\alpha = -1.63$, and generalized Cantor sets with even stronger clustering have $\alpha \to -1$. In this sense, the α value that we obtain for the higher β range (which is more common in *PSP* observations) already represents strong clustering similar to that of the classic Cantor set, while the lower β range has an α value that represents even more extreme clustering of domain boundaries.

In our work, the domain duration distributions at $T_D > T_{D,b}$, above the break duration, also exhibit a power-law form. This indicates scale invariance in the occurrence of domain boundaries, even for time scales longer than the outer scale of the turbulence. We speculate that this could be associated with the scale-invariant $1/f$ noise in the solar wind at low frequency f, which is believed to be driven by solar phenomena (Matthaeus & Goldstein 1986), originating in the lower corona (Bemporad et al. 2008) or possibly deeper in the photosphere or below (Matthaeus et al. 2007).

It is not surprising that plasma β has a strong effect on domains of approximate magnetic pressure balance, with a qualitative difference between solar wind of $\beta < 1$, for which magnetic pressure dominates over plasma pressure, and $\beta \approx 1$, with approximate equipartition between magnetic and plasma energy density and pressure. Previous work has classified the slow solar wind as having two states with different ranges of β (e.g., Griton et al. 2021; D'Amicis et al. 2021). However, we do find it surprising that our results indicate a quantitative, continuous relationship between the mean domain duration $\langle T_D \rangle$ and β (see Figure 8), rather than a step or switching function between two extreme states. Specifically, β has a continuous effect on $\langle T_D \rangle$ values over the range $0.1 < \beta < 2$. The deviation from the overall quantitative trend for some time periods at very low β near E4 and E5 perihelia, during which *PSP* was also near the heliospheric current sheet, invites further investigation.

In addition to the inverse association with β, our results are consistent with the relationship $\langle T_D \rangle \propto 1/V_{rel}$ as expected if the domain duration represents the time to traverse spatial regions, either between boundary surfaces or between a pattern of features that interrupt near constancy of $|\mathbf{B}|$, that are statistically homogeneous and isotropic in shape, and convect past the spacecraft with the solar wind. (The evidence does not specifically indicate such proportionality, but does not rule it out.)

However, the results are inconsistent with the relationships $\langle T_D \rangle \propto 1/V_{\perp rel}$ and $\langle T_D \rangle \propto 1/V'_{\perp rel}$ as expected for convection of such spatial structures if they are highly elongated along the radial or local Parker spiral direction, respectively. This rules out, for example, the interpretation of domain boundaries as solid walls of flux tubes oriented in one of these directions. This does not necessarily conflict with the recent observation that switchback regions are elongated along the Parker spiral direction (Laker et al. 2021). Given that the domain boundaries often include switchbacks, the domains themselves may represent the space between switchbacks, in which case the aspect ratio of domains relates to the spatial patterning of switchback positions rather than the shapes of individual switchback regions.

Indeed, even if coherent structures such as current sheets are believed to relate to a flux tube structure in the solar wind, as suggested many times in the literature (e.g., Bartley et al. 1966; Bruno et al. 2001; Borovsky 2008), 2D MHD simulations of magnetic turbulence have indicated that flux structures do not have well-defined walls densely populated with current sheets; rather, current sheets are sparsely distributed at different nested flux structures (Seripienlert et al. 2010). We speculate that in three dimensions, the locations of current sheets may be sparsely distributed along the flux tube direction as well. This could relieve the tension between observations of flux-tube structuring in the solar wind and the result that domains, related to the spaces between strong coherent magnetic structures, do not exhibit a large aspect ratio along the radial or Parker spiral direction.

Finally, we note that our inference that domains do not represent elongated structures in one of those directions, and could have an isotropic shape, is consistent with the observation from white-light images that solar wind density fluctuations transition from radial "striae"

near the Sun to "flocculae" that are nearly isotropic in the sky plane (DeForest et al. 2016). This transition can be attributed to shear-driven dynamics and nonlinear Kelvin-Helmholtz instabilities near the Alfvén critical zone that energize solar wind turbulence and lead to mixing layer dynamics that tend to isotropize the distribution of coherent structures in the solar wind (Ruffolo et al. 2020). Note that the data analyzed in this work were taken while *PSP* was completely or predominantly outside the Alfvén critical zone (depending on how this is defined; see Figure 9(a) of Ruffolo et al. 2020; Wexler et al. 2021), so spatial domains with an isotropic aspect ratio are consistent with this view.

In conclusion, we have defined and characterized the basic properties of contiguous domains of approximate magnetic pressure balance, i.e., nearly constant $|\mathbf{B}|$, which can be considered as Alfvénic domains. These domains relate to Alfvénic turbulence (Barnes 1979, 1981) and dynamical plasma relaxation processes (Servidio et al. 2008). The domain duration relates to the waiting time between events that disrupt the near constancy of $|\mathbf{B}|$, many of which are switchbacks. The filling fraction of domains, which can serve as a measure of Alfvénicity of extended time periods, has a strong inverse relation with distance r from the Sun over the first five *PSP* orbits. The mean domain duration has a strong and continuous inverse relation with plasma β over $0.1 < \beta < 2$. Domain distributions have a broken power-law form with a break on the order of the turbulence correlation time, and are qualitatively consistent with previously measured waiting time distributions between switchbacks and magnetic PVI events. If domains represent statistically homogeneous spatial structures carried with the solar wind, their shapes are not highly elongated along the radial or Parker spiral direction. These exercises in quantifying statistical properties of near-constant magnitude magnetic domains may help clarify what has been described as a flux tube or spaghetti model (McCracken & Ness 1966; Burlaga 1969; Borovsky 2008, 2016). A goal for the future is to employ these clues and constraints to determine the dynamical origin of this organized, cellular structure of the solar wind magnetic field.

ACKNOWLEDGMENTS

This research has been supported in part by grant RTA6280002 from Thailand Science Research and Innovation and the Parker Solar Probe mission under the ISOIS project (contract NNN06AA01C) and a subcontract to University of Delaware from Princeton University (SUB0000165). Additional support is acknowledged from the NASA LWS program (NNX17AB79G) and the HSR program (80NSSC18K1210 & 80NSSC18K1648).

REFERENCES

Bale, S. D., Goetz, K., Harvey, P. R., et al. 2016, SSRv, 204, 49, doi: 10.1007/s11214-016-0244-5

Bale, S. D., Badman, S. T., Bonnell, J. W., et al. 2019, Nature, 576, 237, doi: 10.1038/s41586-019-1818-7

Barnes, A. 1979, Hydromagnetic waves and turbulence in the solar wind, ed. E. N. Parker, C. F. Kennel, & L. J. Lanzerotti, Vol. 1, 249–319

Barnes, A. 1981, Journal of Geophysical Research, 86, 7498

Barnes, A., & Hollweg, J. V. 1974, J. Geophys. Res., 79, 2302, doi: 10.1029/JA079i016p02302

Bartley, W. C., Bukata, R. P., McCracken, K. G., & Rao, U. R. 1966, J. Geophys. Res., 71, 3297, doi: 10.1029/JZ071i013p03297

Belcher, J. W., & Davis, L., J. 1971, J. Geophys. Res., 76, 3534, doi: 10.1029/JA076i016p03534

Bemporad, A., Matthaeus, W., & Poletto, G. 2008, The Astrophysical Journal Letters, 677, L137

Borovsky, J. E. 2008, Journal of Geophysical Research (Space Physics), 113, A08110, doi: 10.1029/2007JA012684

—. 2016, Journal of Geophysical Research (Space Physics), 121, 5055, doi: 10.1002/2016JA022686

Bruno, R., & Carbone, V. 2013, Living Reviews in Solar Physics, 10, 2, doi: 10.12942/lrsp-2013-2

Bruno, R., Carbone, V., Veltri, P., Pietropaolo, E., & Bavassano, B. 2001, Planet. Space Sci., 49, 1201, doi: 10.1016/S0032-0633(01)00061-7

Bruno, R., D'Amicis, R., Bavassano, B., Carbone, V., & Sorriso-Valvo, L. 2007, Annales Geophysicae, 25, 1913, doi: 10.5194/angeo-25-1913-2007

Burlaga, L. F. 1969, SoPh, 7, 54, doi: 10.1007/BF00148406

Cantor, G. 1883, Mathematische Annalen, 21, 545, doi: 10.1007/BF01446819

Chen, C. H. K., Bale, S. D., Bonnell, J. W., et al. 2020, ApJS, 246, 53, doi: 10.3847/1538-4365/ab60a3

Chhiber, R., Goldstein, M. L., Maruca, B. A., et al. 2020, ApJS, 246, 31, doi: 10.3847/1538-4365/ab53d2

Coleman, Paul J., J. 1968, ApJ, 153, 371, doi: 10.1086/149674

D'Amicis, R., Perrone, D., Bruno, R., & Velli, M. 2021, Journal of Geophysical Research (Space Physics), 126, e28996, doi: 10.1029/2020JA028996

Davies, L., & Gather, U. 1993, Journal of the American Statistical Association, 88, 782, doi: 10.1080/01621459.1993.10476339
DeForest, C. E., Matthaeus, W. H., Viall, N. M., & Cranmer, S. R. 2016, ApJ, 828, 66, doi: 10.3847/0004-637X/828/2/66
Drake, J. F., Agapitov, O., Swisdak, M., et al. 2021, A&A, 650, A2, doi: 10.1051/0004-6361/202039432
Drury, L. O. 1983, Reports on Progress in Physics, 46, 973, doi: 10.1088/0034-4885/46/8/002
Dudok de Wit, T., Krasnoselskikh, V. V., Bale, S. D., et al. 2020, ApJS, 246, 39, doi: 10.3847/1538-4365/ab5853
Fisk, L. A., & Kasper, J. C. 2020, ApJL, 894, L4, doi: 10.3847/2041-8213/ab8acd
Goldstein, M. L., Klimas, A. J., & Barish, F. D. 1974, in Solar Wind Three, ed. C. T. Russell, 385–387
Greco, A., Chuychai, P., Matthaeus, W. H., Servidio, S., & Dmitruk, P. 2008, Geophys. Res. Lett., 35, L19111, doi: 10.1029/2008GL035454
Gringauz, K. I., Bezrokikh, V. V., Ozerov, V. D., & Rybchinskii, R. E. 1960, Soviet Physics Doklady, 5, 361
Griton, L., Rouillard, A. P., Poirier, N., et al. 2021, ApJ, 910, 63, doi: 10.3847/1538-4357/abe309
Horbury, T. S., Woolley, T., Laker, R., et al. 2020, ApJS, 246, 45, doi: 10.3847/1538-4365/ab5b15
Jokipii, J. R. 1966, ApJ, 146, 480, doi: 10.1086/148912
Kasper, J. C., Abiad, R., Austin, G., et al. 2016, SSRv, 204, 131, doi: 10.1007/s11214-015-0206-3
Kasper, J. C., Bale, S. D., Belcher, J. W., et al. 2019, Nature, 576, 228, doi: 10.1038/s41586-019-1813-z
Klein, L., Bruno, R., Bavassano, B., & Rosenbauer, H. 1993, J. Geophys. Res., 98, 17461, doi: 10.1029/93JA01522
Knipp, D. J. 2011, Understanding Space Weather and the Physics Behind It, Space Technology Series (McGraw-Hill). https://spacetechnologyseries.com/books/Space-Weather.html
Kryukov, I. A., Pogorelov, N. V., Zank, G. P., & Borovikov, S. N. 2012, in American Institute of Physics Conference Series, Vol. 1436, Physics of the Heliosphere: A 10 Year Retrospective, ed. J. Heerikhuisen, G. Li, N. Pogorelov, & G. Zank, 48–54, doi: 10.1063/1.4723589
Laker, R., Horbury, T. S., Bale, S. D., et al. 2021, A&A, 650, A1, doi: 10.1051/0004-6361/202039354
Matteini, L., Horbury, T. S., Pantellini, F., Velli, M., & Schwartz, S. J. 2015, ApJ, 802, 11, doi: 10.1088/0004-637x/802/1/11
Matthaeus, W. H., Breech, B., Dmitruk, P., et al. 2007, Astrophys. J. Lett., 657, L121, doi: 10.1086/513075
Matthaeus, W. H., & Goldstein, M. L. 1986, 57, 495, doi: 10.1103/PhysRevLett.57.495
McCracken, K., & Ness, N. 1966, Journal of Geophysical Research, 71, 3315
Meyer, P., Parker, E. N., & Simpson, J. A. 1956, Physical Review, 104, 768, doi: 10.1103/PhysRev.104.768
Moffatt, H. K. 1978, Magnetic field generation in electrically conducting fluids
Mozer, F. S., Agapitov, O. V., Bale, S. D., et al. 2020, ApJS, 246, 68, doi: 10.3847/1538-4365/ab7196
Neugebauer, M., & Snyder, C. W. 1962, Science, 138, 1095, doi: 10.1126/science.138.3545.1095-a
Parashar, T. N., Goldstein, M. L., Maruca, B. A., et al. 2020, ApJS, 246, 58, doi: 10.3847/1538-4365/ab64e6
Parker, E. N. 1958, ApJ, 128, 664, doi: 10.1086/146579
Pine, Z. B., Smith, C. W., Hollick, S. J., et al. 2020, ApJ, 900, 93, doi: 10.3847/1538-4357/abab11
Rouillard, A. P., Kouloumvakos, A., Vourlidas, A., et al. 2020, ApJS, 246, 37, doi: 10.3847/1538-4365/ab579a
Ruffolo, D., Matthaeus, W. H., Chhiber, R., et al. 2020, ApJ, 902, 94, doi: 10.3847/1538-4357/abb594
Schwadron, N. A., & McComas, D. J. 2021, ApJ, 909, 95, doi: 10.3847/1538-4357/abd4e6
Seripienlert, A., Ruffolo, D., Matthaeus, W. H., & Chuychai, P. 2010, ApJ, 711, 980, doi: 10.1088/0004-637X/711/2/980
Servidio, S., Matthaeus, W. H., & Dmitruk, P. 2008, 100, doi: 10.1103/PhysRevLett.100.095005
Shiota, D., Zank, G. P., Adhikari, L., et al. 2017, ApJ, 837, 75, doi: 10.3847/1538-4357/aa60bc
Sittkus, A. 1956, Zeitschrift Naturforschung Teil A, 11, 604, doi: 10.1515/zna-1956-0711
Smith, C. W., Vasquez, B. J., & Hamilton, K. 2006, 111, A09111, doi:10.1029/2006JA011651, doi: 10.1029/2006JA011651
Squire, J., Chandran, B. D. G., & Meyrand, R. 2020, ApJL, 891, L2, doi: 10.3847/2041-8213/ab74e1
Telloni, D., Sorriso-Valvo, L., Woodham, L. D., et al. 2021, ApJL, 912, L21, doi: 10.3847/2041-8213/abf7d1
Usmanov, A. V., Matthaeus, W. H., Breech, B., & Goldstein, M. L. 2009, in Astronomical Society of the Pacific Conference Series, Vol. 406, Numerical Modeling of Space Plasma Flows: ASTRONUM-2008, ed. N. V. Pogorelov, E. Audit, P. Colella, & G. P. Zank, 160
Walén, C. 1944, Arkiv for Matematik, Astronomi och Fysik, 30A, 1
Wexler, D. B., Stevens, M. L., Case, A. W., & Song, P. 2021, ApJL, 919, L33, doi: 10.3847/2041-8213/ac25fa
Wiengarten, T., Fichtner, H., Kleimann, J., & Kissmann, R. 2015, ApJ, 805, 155, doi: 10.1088/0004-637X/805/2/155

Zank, G. P., Nakanotani, M., Zhao, L. L., Adhikari, L., & Kasper, J. 2020, ApJ, 903, 1, doi: 10.3847/1538-4357/abb828